

Original Research

Acupoint Catgut Embedding Diminishes Fibromyalgia Pain through TRPV1 in the Mouse Brain

Po-Chih Lai¹, Chia-Ming Yen^{2,3}, I-Han Hsiao⁴, Yung-Hsiang Chen⁵, Yi-Wen Lin^{1,6,*}¹College of Chinese Medicine, Graduate Institute of Acupuncture Science, China Medical University, 404332 Taichung, Taiwan²Department of Anesthesiology, Taichung Tzu Chi Hospital, Buddhist Tzu Chi Medical Foundation, 42743 Taichung, Taiwan³School of Post-Baccalaureate Chinese Medicine, Tzu Chi University, 97004 Hualien, Taiwan⁴Department of Neurosurgery, China Medical University Hospital, 404332 Taichung, Taiwan⁵Graduate Institute of Integrated Medicine, China Medical University, 404332 Taichung, Taiwan⁶Chinese Medicine Research Center, China Medical University, 404332 Taichung, Taiwan*Correspondence: yiwlin@mail.cmu.edu.tw (Yi-Wen Lin)

Academic Editor: Gernot Riedel

Submitted: 13 April 2023 Revised: 9 May 2023 Accepted: 12 May 2023 Published: 17 July 2023

Abstract

Background: Chronic pain refers to pain that persists for over three months. Chronic pain may restrict activities of daily living, including work, learning, social life, and can lead to anxiety, depression, and sleep disturbance. Imaging data have demonstrated that central sensitization often occurs in the brain of patients with chronic pain, which arises from imbalanced neurotransmission in the central nervous system. Transient receptor potential vanilloid 1 (TRPV1) is an ion channel to serve as an inflammatory detector in the brain. We aim to determine the properties of acupoint catgut embedding (ACE) on cold stress-induced mice fibromyalgia (FM) and surveyed the character of TRPV1 and linked molecules in chronic FM pain. **Methods:** Intermittent cold stress (ICS) was used to induce mice FM model. Mice were subgrouped into normal mice, ICS-induced FM group, FM mice with ACE, and FM in *Trpv1*^{-/-} group. ACE is a novel acupuncture technique that provides convenience and continuous nerve stimulation that has been reported effective on pain management. **Results:** Our behavioral experiments showed similar levels of pain response among all groups before treatment. After ICS, prolonged mechanical and thermal pain was initiated (mechanical threshold: 1.96 ± 0.12 g; thermal latency: 4.86 ± 0.21 s) and were alleviated by ACE treatment and *TRPV1* gene deletion. Inflammatory mediators were increased in the plasma of FM mice, while TRPV1 and related kinases were amplified in the hypothalamus and cerebellum. These changes were ameliorated in the ACE-treated and *Trpv1*^{-/-} groups. **Conclusions:** These novel findings suggest that chronic FM pain can be modulated by ACE or *TRPV1* gene deletion. The analgesic effect of ACE through the TRPV1 pathway may reflect its potential as a therapeutic target for FM treatment.

Keywords: fibromyalgia; acupoint catgut embedding; TRPV1; phosphorylated endoplasmic reticulum kinase (pERK); medial prefrontal cortex (mPFC); somatosensory (SSC)

1. Introduction

Acute pain typically accompanies injury, such as wounds, tissue damage, or fractures. Various pharmacological agents are available to relieve acute pain. In contrast, chronic pain persists long after recovery from the injury or damage. About 1/4 of adults suffer from chronic pain, identified as discomfort sustained for over three months, and accounts for a high proportion of insurance claims [1]. Chronic pain can result from various etiologies including arthritis, cancer pain, low back pain, headaches, muscle pain, and fibromyalgia (FM). FM is presently described as a complex disease characterized by chronic widespread muscle pain, fatigue, insomnia, anxiety, and depression [2]. FM is a growing issue affecting individuals, insurance providers, healthcare systems, economies, and societies. There are no curative therapies for FM and methods to relieve FM pain are lacking due to its unclear fundamental mechanisms. The occurrence of FM is around 2–8% of people, depending on the analytic principles used [2]. New di-

agnostic principles for FM to include widespread pain index (WPI) and symptom severity scale (SS). The WPI examines 19 common body pain parts for two weeks. The SS calculates the degree of fatigue, waking, and cognitive symptoms. FM is characterized as $WPI \geq 7$ and $SS \geq 5$ or $WPI 3-6$ and $SS \geq 9$ in the last three months. Recently, three medications of FM were permitted by the U.S. Food and Drug Administration (FDA), including duloxetine (Cymbalta), milnacipran (Savella), and pregabalin (Lyrica) [3–5].

Acupuncture is an ancient Chinese medicine technique that involves implanting a steel needle into an acupoint. Acupuncture is helpful in managing FM due to its ability to reduce pain, anxiety, depression, and insomnia [6,7]. In addition, electroacupuncture (EA) has been described to attenuate numerous kinds of pain [8–12]. Recently, acupoint catgut embedding (ACE) was developed as a novel technique to establish constant acupoint stimulation. ACE treatment has been shown to be more effective and its benefits prolonged than acupuncture or EA in man-



aging obesity [13]. ACE has the advantages of long-term effects and low cost, and has been broadly utilized in the management of acute or chronic pain [14,15]. Recent articles showed that ACE activates the immune system because the absorbable chromic catgut sutures are recognized as a non-self protein [16]. ACE can induce long-term immune responses such as macrophage phagocytosis and neutrophil infiltration [17]. ACE can also reliably diminish postoperative pain and decrease analgesic medicine intake [18].

Transient Receptor Potential Vanilloid (TRPV) is an ion channel chiefly located on the neuronal membrane. TRPV can be activated by vanilloid compounds and has six subtypes. TRPV1 was first recognized as a receptor of capsaicin, the major constituent of chili pepper [19]. TRPV1 exists in the dorsal root ganglion, spinal cord, and trigeminal ganglion for pain sensation and transmission. In peripheral regions, TRPV1 greatly exists in A- and C-type sensory neurons to detect inflammation and painful stimuli. TRPV1 was also described to exist in the central nerve system (CNS) for thermoregulation, synaptic transmission, and detection of inflammation [19]. Furthermore, TRPV1 is expressed in non-neuronal astrocytes or glial cells for pain signaling [20]. TRPV1 is expressed in several brain areas including thalamus, somatosensory cortex, prefrontal cortex, hippocampus, amygdala, hypothalamus (Hypo), and cerebellum (CB). TRPV1 activation sequentially activates kinases, such as protein kinase A (PKA), phosphoinositide 3-kinases (PI3K), protein kinase C (PKC), and Ca^{2+} /calmodulin-dependent kinase II (CaMKII) [21,22]. Furthermore, these kinases then trigger mitogen-activated protein kinase (MAPK), pAkt, pmTOR, and further increase transcriptional factors, such as cAMP-response element binding protein (CREB) and nuclear factor kappa-light-chain-enhancer of activated B cells ($\text{NF}\kappa\text{B}$). These kinases also play a role in sensitizing peripheral afferents resulting in mechanical and thermal hyperalgesia [21,22]. A recent article indicated that immune cells release several factors to activate individual receptors on the membrane of the nerve terminals during pain development and treatment [23].

The plan of the current study was to verify our hypotheses that FM is related to augmenting TRPV1 signaling in the mouse brain and that ACE ameliorates both mechanical and thermal nociception through suppression of TRPV1 pathway. To address these questions, we used a mouse FM through intermittent cold stress (ICS). Consistent with our hypothesis, mice subjected to ICS exhibited significant chronic mechanical and thermal pain that could be abridged by ACE or *TRPV1* gene deletion. TRPV1 pathway was amplified in the mouse Hypo and CB and can be relieved by ACE and *TRPV1* gene loss. These data suggest the therapeutic effect of ACE is connected with TRPV1 in the mouse brain. We propose that the TRPV1 signaling pathway is a potential target for FM treatment.

2. Materials and Methods

2.1 Experimental Animals

The treatment of mice was permitted by China Medical University Committee (CMUIACUC-2022-424), Taiwan, subsequent the guideline for the practice of experimental animals (National Academy Press). The current work is indicated according to the ARRIVE guidelines. Totally, 40 female mice were used in the current study, containing 30 normal mice (BioLASCO, Co., Ltd, Taipei, Taiwan) and 10 *Trpv1*^{-/-} mice. The animals were hosted in the experimental animal center (12/12 h) with all diet and water provided free. The estimated model size of 10 mice in each group was designed for an α value of 0.05 with the influence of 80%. Mice used in the present study and their misery were minimalized. The experimental staffs were blind to group distribution through the examinations. Animals were further subgrouped into four groups: Normal mice (Group 1: Normal); ICS-initiated FM group (Group 2: FM); FM cured with ACE group (Group 3: FM + ACE), and FM in *Trpv1*^{-/-} group (Group 4: FM + *Trpv1*^{-/-}).

2.2 FM Induction and Multiplex Enzyme-Linked Immunosorbent Assay

All animals were accommodated at 24 ± 1 °C before FM induction. In this ICS model, the animals were placed at ± 1 °C temperature overnight (starting from 4 PM–10 AM). Animals were next transported to 24 ± 1 °C temperature for a 30-minute duration in the next morning. The animals were further relocated back to 4 ± 1 °C temperature for another 30 minutes. The challenge of environmental temperatures induced a murine FM model. Normal mice were placed in the same place at room temperature. After all experimental treatment of FM at day 14, the mice plasma was collected by retro-orbital sinus puncture and examined through examined multiplex enzyme-linked immunosorbent assay (ELISA: lot. MA1M191126, Quansys Biosciences, Logan, UT, USA) through Q-view 1.5 (Quansys Biosciences, Logan, UT, USA).

2.3 ACE Treatment

ACE mice had received ACE treatment at the bilateral stomach 36 (ST36) acupoint at days 0 and 7. Like human anatomy, the ST36 acupoint is sited longitudinally at 3 mm under the apex of patella bone intersecting horizontally 1 mm lateral to anterior the tibia bone at the central of the tibialis anterior muscle. Sterilized needle 0.6×25 mm (160925, Terumo Corporation, Tokyo, Japan), steel needle 0.35×40 mm (Suzhou Medical Appliance, Suzhou, China), or catgut suture 0.2×4 mm (CP Medical Inc, Norcross, GA, USA) were utilized for ACE. Mice were engaged into a chamber for anesthesia. Both ST36 acupoints were decontaminated with 75% alcohol and the commercial syringe needle was implanted, followed by the catgut inserted at the 5 mm depth.

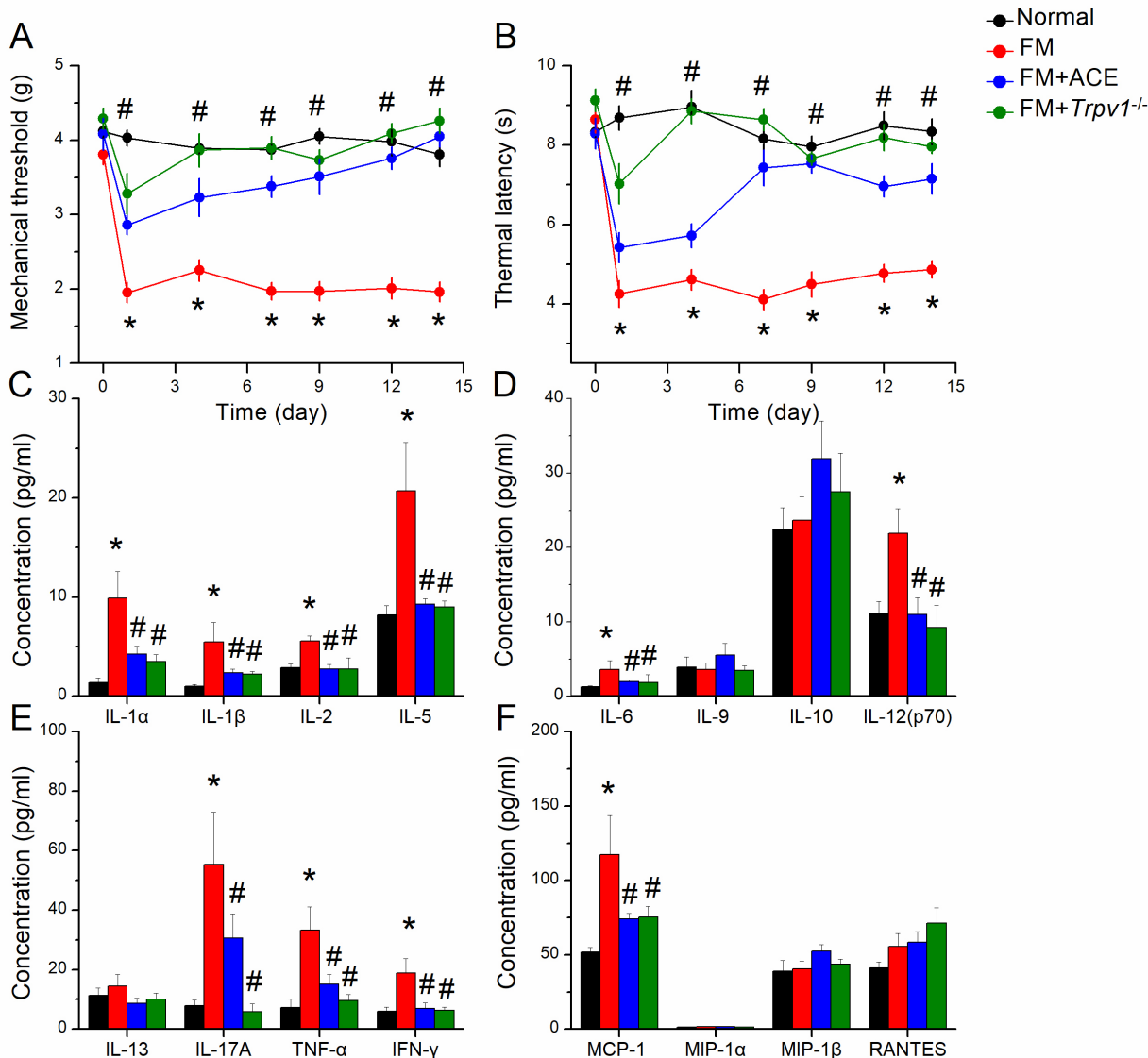


Fig. 1. Mechanical, thermal pain, and inflammatory cytokines in normal, FM, FM+ACE, and FM+Trpv1^{-/-} groups. (A) Mechanical force obtained via von Frey examinations. (B) Thermal time observed via the Hargreaves' test. (C) IL-1α, IL-1β, IL-2, IL-5. (D) IL-6, IL-9, IL-10, IL-12(p70). (E) IL-13, IL-17A, TNF-α, IFN-γ. (F) MCP-1, and MIP-1α. MIP-1β, RANTES. *shows statistical differences compared with normal mice. #shows statistical differences compared with FM groups. n = 10 in four groups. FM, fibromyalgia; ACE, acupoint catgut embedding; Trpv1, Transient receptor potential vanilloid 1.

2.4 Pain Behavior Test

Mechanical or thermal nociceptive performances were measured 7 periods from day 0 to 14 after FM induction. We first verified the von Frey filament examination, mechanical pain was tested by calculating the strength of replies to stimuli within 3 performances of von Frey test (IITC Life Science Inc, Los Angeles, CA, USA). Animals were then placed to a steel net (75 × 25 × 45 cm) and then quarantined under plastic cage (10 × 6 × 11 cm). Animals were examined with von Frey at center plantar of hind paw. The values were calculated as gram and were documented when the mice withdraw the paw. Besides, the Hargreaves' examination was achieved to quantify the thermal hyperal-

gesia via conniving the latency to thermal stimuli with three tests through Hargreaves' test (IITC Life Sciences, Los Angeles, CA, USA). Animals were then engaged in a flexible cage on the top of IITC analgesimeter. The thermal examiner was placed under the IITC analgesimeter. Animals were placed to the behavior room for more than 30 minutes earlier examinations. The tests were performed when the individuals were quiet rather than grooming or sleeping.

2.5 Western Blot Analysis

Animals were sedated under isoflurane and suffered cervical dislocation. Mice Hypo and CB samples were separated to draw out proteins and further kept at -80 °C re-

Hypo

C

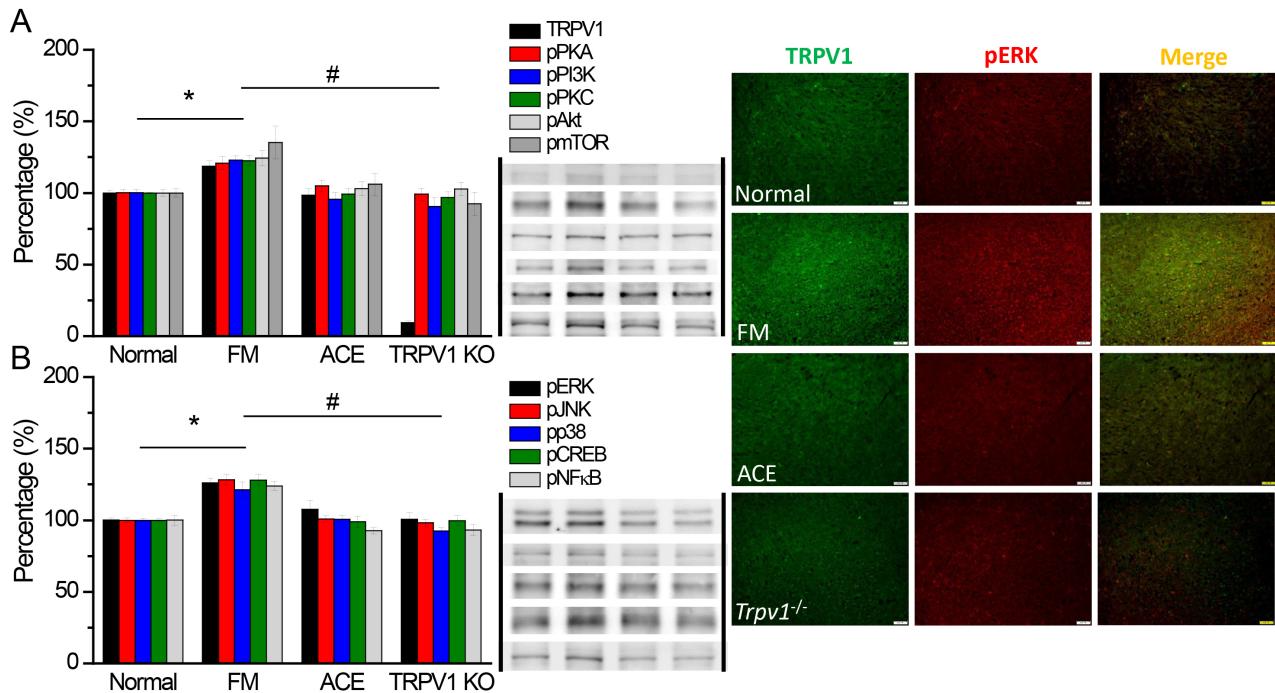


Fig. 2. TRPV1 and linked kinases in the mice hypothalamus. The western blot signals of Normal, FM, ACE, and *Trpv1*^{-/-}. (A) TRPV1, pPKA, pPI3K, pPKC, pAkt, and pmTOR. (B) pERK, pp38, pJNK, pCREB, and pNFκB. *shows statistical differences compared with normal mice. #shows statistical differences compared with FM groups. n = 10 in four groups. n = 6 in four groups. (C) Immunofluorescence signals of TRPV1, pERK, or colocalized labeling in the mice hypothalamus (green, red or yellow). Scale bar = 100 μm. n = 4 in four groups.

refrigerator for protein mining. All extracted samples were standardized with radioimmunoprecipitation (RIPA) with: 1% NP-40, 50 mM Tris-HCl, 0.02% NaN₃, 250 mM NaCl, 1 mM Na₃VO₄, 5 mM EDTA, 50 mM NaF, and 1× protease blocker set (AMRESCO, Radnor, PA, USA). Total components were undergoing 8% SDS-Tris electrophoresis and conveyed to commercial polyvinylidene difluoride (PVDF). The membrane was rinsed with 3% bovine serum albumin (BSA, Merck, St. Louis, MO, USA) in TBS-T buffer (100 mM NaCl, 10 mM Tris pH 7.5, 0.1% Tween 20), nurtured with a primary antibody in TBS-T for 1 hour against anti-tubulin (~55 kDa, 1:5000, Merck, St. Louis, MO, USA), TRPV1 (~95 kDa, 1:1000, Alomone, Jerusalem, Israel), pPKA (~40 kDa, 1:1000, Alomone, Jerusalem, Israel), pPKC (~100 kDa, 1:1000, Millipore, St. Louis, MO, USA), pPI3K (~125 kDa, 1:1000, Millipore, St. Louis, MO, USA), pERK1/2 (~42–44 kDa, 1:1000, Millipore, St. Louis, MO, USA), pp38 (~41 kDa, 1:1000, Millipore, St. Louis, MO, USA), pJNK (~42 kDa, 1:1000, Millipore, St. Louis, MO, USA), pAkt (~60 kDa, 1:1000, Millipore, St. Louis, MO, USA), pmTOR

(~180 kDa, 1:500, Millipore, St. Louis, MO, USA), pNFκB (~65 kDa, 1:1000, Millipore, St. Louis, MO, USA), and pCREB (~55 kDa, 1:1000, Millipore, St. Louis, MO, USA) in TBS-T (1% BSA). The PVDF membranes were then edited for incubation with individual antibodies. Peroxidase-conjugated anti-mouse, anti-rabbit, or anti-goat antibodies (1:5000) were utilized as a secondary antibody (Merck, St. Louis, MO, USA). The western blot signals were imaged with improved chemiluminescent (PIERCE) with LAS-3000 Fujifilm (Fuji Photo Film Co., Ltd., Tokyo, Japan). Visible bands concentrations of precise molecular weight were counted with Image J software (NIH, Bethesda, MD, USA). The β-actin band was used as control.

2.6 Immunofluorescence

Animals had been anaesthetized with isoflurane and intracardially filled with 0.9% normal saline and then 4% paraformaldehyde. The mice brain was instantly cut apart and next fixed with 4% paraformaldehyde in refrigerator for 2–3 days. The brains were next engaged in 30% sucrose in 4

CB5

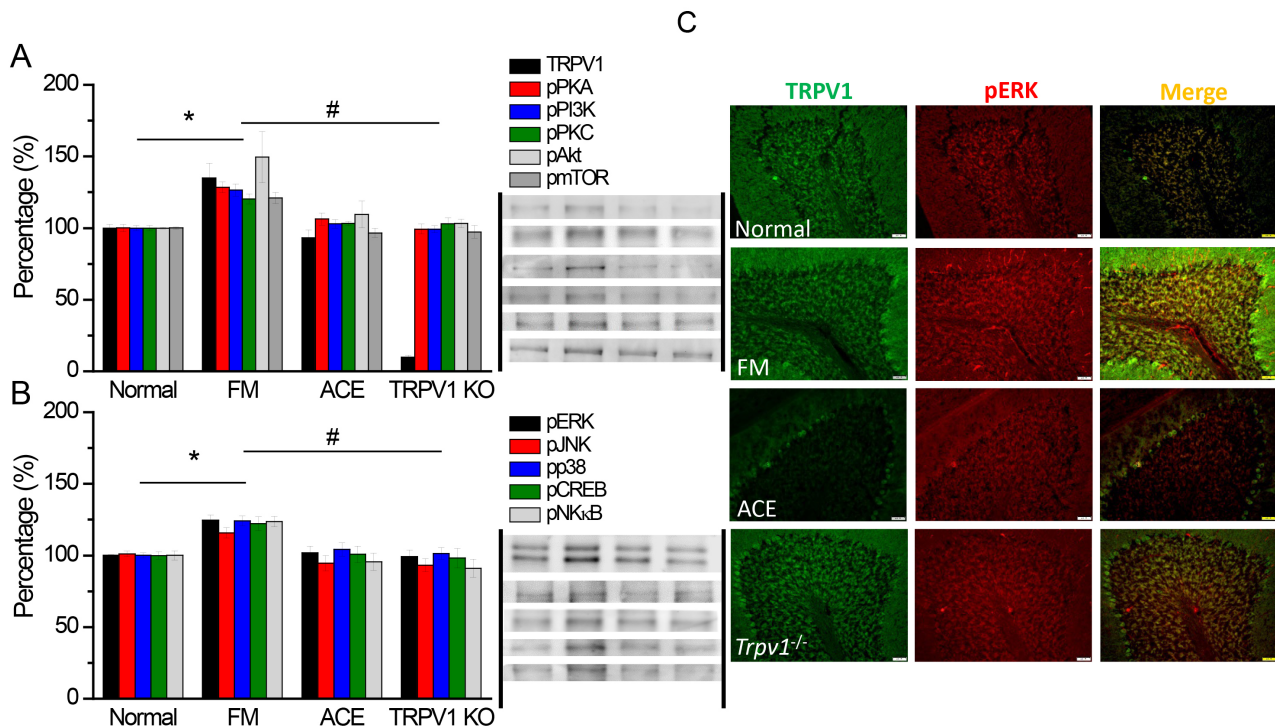


Fig. 3. The intensities of TRPV1 and associated factors in CB5. The western blot signals of Normal, FM, FM+ACE, and *Trpv1*^{-/-} groups. We found intensifications of (A) TRPV1, pPKA, pPI3K, pPKC, pAkt, and pmTOR. (B) pERK, pp38, pJNK, pCREB, and pNFκB. *shows statistical differences compared with normal mice. #shows statistical differences compared with FM groups. n = 10 in four groups. n = 6 in all groups. (C) Immunofluorescence labeling of TRPV1, pERK, and colocalized labeling in CB5 (green, red or yellow). Scale bar = 100 μm. n = 4 in four groups.

°C refrigerator for 2–3 days. The mice tissue was fixed with optimal cutting temperature compound and quickly stored at -80 °C refrigerator. Mice brains were sliced and then placed on glass slides (20 μm). The tissues were further rinsed with 3% BSA, 0.1% Triton X-100, and 0.02% NaN₃ (1 h). The tissues were then nurtured through the first antibody (1:100, Alomone, Jerusalem, Israel), anti-TRPV1 or anti-phosphorylated endoplasmic reticulum kinase (pERK) primed in 1% BSA in 4 °C refrigerator. Tissue slices were further nurtured with the secondary antibody (1:500), 488-conjugated AffiniPure donkey anti-rabbit IgG (Merck, St. Louis, MO, USA), 594-conjugated AffiniPure donkey anti-goat IgG (Merck, St. Louis, MO, USA) for 2 h at room temperature. The tissues were further examined with a microscope (BX-51, Olympus, Tokyo, Japan) with 20 × objective. The photos were examined with Image J software (NIH, Bethesda, MD, USA).

2.7 Statistical Analysis

Statistical differences were accomplished by using the SPSS software (SPSS 21, IBM Corp., Chicago, IL, USA).

All results are offered as the mean with standard error (SEM). Shapiro-Wilk examination was achieved to examination the familiarity of results. Statistical differences in four groups were confirmed via the analysis of variance (ANOVA) test and a post hoc Tukey's test. $p < 0.05$ were identified as statistical differences.

3. Results

3.1 ICS Induced Mechanical and Thermal Chronic Pain Which Could Be Relieved by ACE or TRPV1 Gene Loss

We induced a mice FM and determined their analgesic outcome of ACE and *TRPV1* gene deletion. All mice showed similar mechanical threshold tendencies, which was normally distributed at baseline and was not statistically different among all groups. Cold stress reliably induced mechanical hyperalgesia (Fig. 1A, red circle, D14: 1.96 ± 0.13 , * $p < 0.05$, n = 10) via von Frey filament test. Mechanical hyperalgesia was markedly alleviated by ACE treatment and TRPV1 gene deletion (Fig. 1A, blue and green circles, D14: 4.05 ± 0.14 and 4.26 ± 0.17 , # $p < 0.05$, n = 10, respectively). ICS also induced thermal hyperalge-

CB6

C

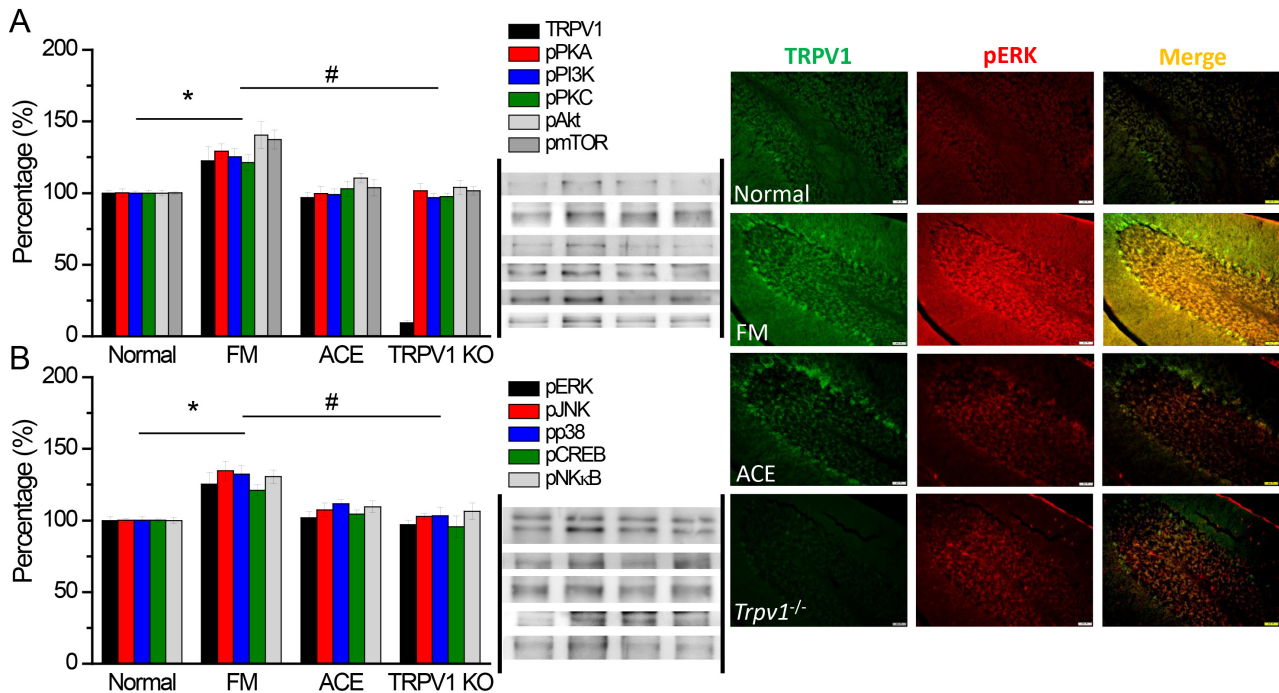


Fig. 4. TRPV1 and associated kinases in CB6. The western blot signals of Normal, FM, FM+ACE, and *Trpv1*^{-/-}. (A) TRPV1, pPKA, pPI3K, pPKC, pAkt, and pmTOR. (B) pERK, pp38, pJNK, pCREB, and pNFκB. *shows statistical differences compared with normal mice. # shows statistical differences compared with FM groups. n = 10 in four groups. n = 6 in all groups. (C) Immunofluorescence labeling of TRPV1, pERK, and colocalized labeling in CB6 (green, red or yellow). Scale bar = 100 μm. n = 4 in four groups.

sia, as observed in the Hargraves' test (Fig. 1B, red circle, D14: 4.86 ± 0.2 , * $p < 0.05$, n = 10). Furthermore, ACE decreased thermal hyperalgesia in the FM mice (Fig. 1B, blue and green circles, D14: 7.15 ± 0.38 and 7.96 ± 0.17 , # $p < 0.05$, n = 10, respectively).

3.2 Inflammatory Cytokines Intensely Augmented in the FM Mice and Can Be Alleviated by ACE Treatment or TRPV1 Gene Loss

Neuroinflammation was detected in the blood and cerebral spinal fluid in FM patients. Accordingly, we determined the concentration of inflammatory cytokines in mouse plasma through multiplex ELISA technique. We measured interleukin-1 alpha (IL-1α), IL-1β, IL-2, IL-5, IL-6, IL-9, IL-10, IL-12(p70), IL-13, IL-17A, tumor necrosis factor alpha (TNF-α), interferon gamma (IFN-γ), monocyte chemoattractant protein 1 (MCP-1), macrophage inflammatory protein 1 alpha (MIP-1α), MIP-1β, and regulated on activation, normal T cell expressed and secreted (RANTES). Inflammatory cytokines were low in normal mice at basal conditions. IL-1α, IL-1β, IL-2, IL-5, IL-6, IL-12, IL-17A, TNF-α, IFN-γ, and MCP-1 were increased

at 14 days after FM induction (Fig. 1C–F, red column, * $p < 0.05$, n = 10). ACE meaningfully reduced inflammatory cytokines levels (Fig. 1C–F, blue column, # $p < 0.05$, n = 10). These cytokines were next reduced in *Trpv1*^{-/-} group (Fig. 1C–F, # $p < 0.05$, n = 10, green column).

3.3 Antinociceptive Effect of ACE or TRPV1 Gene Deletion Involved TRPV1 in the Mice Hypothalamus

Hypothalamic dysfunction was reported in FM patients. We performed Western blot to count the protein intensities of molecules in the TRPV1 in the mice hypothalamus. The level of TRPV1 was detected in mice hypothalamus and increased in FM mice (Fig. 2A, black column, * $p < 0.05$, n = 6). Further data showed that ACE reliably reversed the overexpression of TRPV1 (Fig. 2A, black column, # $p < 0.05$, n = 6). TRPV1 was disappeared in hypothalamus of *Trpv1*^{-/-} mice. The level of pPKA, pPI3K, and pPKC were amplified in FM group (Fig. 2A, * $p < 0.05$, n = 6) and were reduced by ACE treatment or TRPV1 gene deletion (Fig. 2A, # $p < 0.05$, n = 6). The level of pAkt and pmTOR were increased in the hypothalamus (Fig. 2A, * $p < 0.05$, n = 6) but decreased in AC-treated and *Trpv1*^{-/-}

mice (Fig. 2A, # $p < 0.05$, $n = 6$). A similar pattern regarding pERK, pp38, and pJNK was also observed in the FM mice. By contrast, this increase was attenuated in mice treated with ACE or *Trpv1*^{-/-} mice (Fig. 2B, # $p < 0.05$, $n = 6$). pCREB and pNF κ B were both increased in the mouse hypothalamus (Fig. 2B, * $p < 0.05$, $n = 6$) and were reduced by ACE or *TRPV1* gene loss (Fig. 2B, # $p < 0.05$, $n = 6$).

We next used immunofluorescence staining to measure TRPV1 in the hypothalamus. We detected low levels of TRPV1 in normal mice and increased levels in FM mouse hypothalamus (Fig. 2C, green color, $n = 4$). ACE and TRPV1 loss consistently abolished the augmentation of TRPV1 (Fig. 2C, green color, $n = 4$). A similar tendency was also observed in pERK appearance (Fig. 2C, red color, $n = 4$). TRPV1 and pERK colocalization increased in the FM mice but was diminished in ACE and *Trpv1*^{-/-} mice (Fig. 2C, yellow color, $n = 4$).

3.4 ACE or Loss of TRPV1 Attenuated FM through TRPV1 in the Mouse CB5

We investigated protein levels in the CB5. TRPV1 protein was significantly augmented after FM induction (Fig. 3A, * $p < 0.05$, $n = 6$). In contrast, it was diminished by ACE handling and *TRPV1* gene deletion, compared to the FM group. (Fig. 3A, # $p < 0.05$, $n = 6$). We observed similar overexpression patterns of pPKA, pPI3K, and pPKC compared to the normal group that was attenuated in the ACE and *Trpv1*^{-/-} individuals (Fig. 3A, # $p < 0.05$, $n = 6$). pERK, pp38, pJNK, pCREB, and pNF κ B levels were amplified after FM induction in the CB5 region (Fig. 3B, * $p < 0.05$, $n = 6$). These effects were relieved after ACE treatment or *TRPV1* gene deletion (Fig. 3B, # $p < 0.05$, $n = 6$). Using immunofluorescence, we showed TRPV1 is expressed in the CB5 of normal mice. TRPV1 was increased after FM induction in the mouse CB5 (Fig. 3C, green color, $n = 4$). The level was then reduced by ACE and TRPV1 gene deletion groups (Fig. 3C, green, $n = 4$). A comparable finding was perceived for pERK (Fig. 3C, red color, $n = 4$). Colocalization of overexpressed TRPV1 or pERK had been detected in the CB5 of FM mice (Fig. 3C, yellow color, $n = 4$). The amplified pattern was decreased in ACE or TRPV1 groups (Fig. 3C, yellow color, $n = 4$).

3.5 Increased TRPV1 Pathway Occurred in FM Mouse CB6 and CB7 that Can Be Reduced by ACE Treatment and TRPV1 Gene Loss

Our data determined the TRPV1 and correlated kinases in the CB6 and CB7 in mice. TRPV1 proteins were significantly augmented after FM stimulation, compared with normal mice (Figs. 4,5A, black column, * $p < 0.05$, $n = 6$). TRPV1 proteins were reduced in the ACE group and were not detected in *Trpv1*^{-/-} mice (Figs. 4,5A, black column, # $p < 0.05$, $n = 6$). FM mice showed augmented pPKA, pPI3K, or pPKC protein in the CB6 and CB7 (Figs. 4,5A, * $p < 0.05$, $n = 6$). These proteins were reduced in the

EA and *Trpv1*^{-/-} groups (Figs. 4,5A, # $p < 0.05$, $n = 6$). Similar results were observed for pAkt-pmTOR molecules (Figs. 4,5A, * $p < 0.05$, $n = 6$). EA and *Trpv1*^{-/-} also reduced aforementioned molecules (Figs. 4,5A, # $p < 0.05$, $n = 6$). Overexpression of pERK, pp38, and pJNK was obtained in FM group (Figs. 4,5B, * $p < 0.05$, $n = 6$) and was abrogated by EA and TRPV1 loss (Figs. 4,5B, # $p < 0.05$, $n = 6$). Our data specified a similar profile for the expression of pCREB and pNF κ B (Figs. 4,5B, * $p < 0.05$, $n = 6$).

We used immunofluorescence to determine the localization of TRPV1 and pERK in CB6 and CB7 following FM induction. TRPV1 levels were significantly increased in the CB6 and CB7 in FM mice (Figs. 4,5C, green fluorescence, $n = 4$), while the result was diminished in the ACE and *Trpv1*^{-/-} groups (Figs. 4,5C). These expression profiles were also observed for pERK (Figs. 4,5C, red fluorescence, $n = 4$). A parallel trend was similarly detected for TRPV1 and pERK colocalization (Figs. 4,5C, yellow fluorescence, $n = 4$).

4. Discussion

We reveal that the FM model mimics the clinical symptoms of chronic mechanical and thermal nociception in FM mice. We then presented that ACE at ST36 site reliably attenuated either mechanical or thermal pain. Similar decreases in pain-related behaviors were also found in mice lacking TRPV1 receptors. TRPV1 and related kinases were all increased in the mice Hypo and CB, which are brain areas involved in pain modulation. These molecules were sequentially diminished by ACE and *TRPV1* gene deletion, signifying that the therapeutic effect of ACE is linked with TRPV1 in the mice Hypo and CB. Our data provide suggestion that TRPV1 signaling pathway molecules could potentially be beneficial targets for FM treatment.

Peripheral nerve stimulation (PNS) is extensively used in several clinical scenarios, especially for pain control. ACE shares similar effects as PNS and transcutaneous electrical nerve stimulation for chronic pain management. PNS is utilized in several chronic pain situations, such as peripheral nerve injury, local pain syndrome, and FM [24,25]. Gilmore *et al.* [26] reported that chronic neuropathic pain is an underdiagnosed nociceptive condition following elimination. They verified the possibility of inserting fine-wire PNS inserts into the sciatic and femoral nerves for pain control. They suggest that PNS may deliver noteworthy pain assistance and facilitate recovery in chronic neuropathic pain patients. They also showed that 60-day PNS stimulation achieves continuous control of chronic pain [26]. A recent article showed that PNS works through both peripheral and central mechanisms. In its central mechanism, PNS can activate dorsal horn interneurons to block pain signals, attenuating central sensitization and hyperalgesia. In the spinal cord, PNS may increase the release of neurotransmitters, including Gamma-aminobutyric acid (GABA), glycine, serotonin, and cannabinoid pathways

CB7

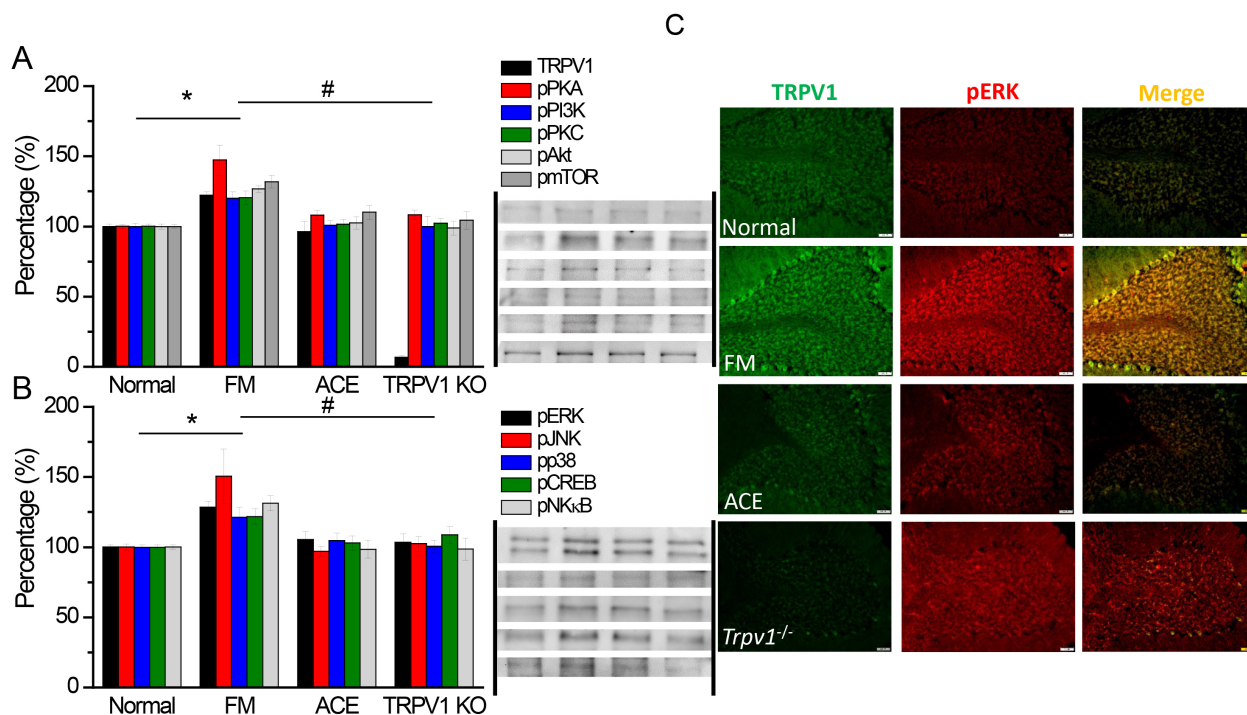


Fig. 5. TRPV1 and associated kinases in CB7. The western blot signals of Normal, FM, FM+ACE, and *Trpv1*^{-/-}. (A) TRPV1, pPKA, pPI3K, pPKC, pAkt, and pmTOR. (B) pERK, pp38, pJNK, pCREB, and pNFκB. *shows statistical differences compared with normal mice. #shows statistical differences compared with FM groups. n = 10 in four groups. n = 6 in four groups. (C) Immunofluorescence staining of TRPV1, pERK, and double staining in the mice CB7 (green, red or yellow). Scale bar = 100 μm. n = 4 in four groups.

[27]. PNS in peripheral sites can attenuate nociceptive afferent signals via changes in the local microenvironment, decrease in neurotransmitters and inflammatory cytokines, and frequency of neural discharge [28,29].

Cui *et al.* [30] showed that ACE can alleviate the over-expression of N-methyl-D-aspartate receptor (NMDA), pCaMKII, pERK, and pCREB by CFA-treated rats. The shot of the serotonin 1A receptor agonist mimicked the properties of ACE and was further blocked by the serotonin 1A receptor blocker WAY-100635 [30]. Du *et al.* [31] reported that ACE has analgesic effects measured as withdrawal thresholds and can decrease paw edema in a mouse inflammatory pain model. ACE markedly ameliorated the increased protein level of the sigma receptor in the mouse lumbar spinal cord. ACE also attenuated the increase in pERK and pp38, and injection of the sigma receptor agonist PRE084 significantly reversed the phenomena [31]. Our recent publications show that EA can relieve mice FM pain through TRPV1 pathway [8,10]. The current study further determined that ACE has an analgesic effect through suppression of TRPV1 activity similar to EA. These results indicate the beneficial effect of ACE for continuous and prolonged treatment for FM.

Recently, we showed that EA can relieve both acute and chronic pain through the TRPV1 pathway. In this study, we provide evidence that cold stress chronic pain may be associated with increased TRPV1 in the mouse brain and that ACE exerts its analgesic effect via suppression of TRPV1 activity in these areas. To address this issue, we induced chronic pain by cold stress and observed pain-related behaviors in mice. Consistent with our hypothesis, cold stress meaningfully convinced mechanical and thermal hyperalgesia, and ACE reliably reversed this nociception. In addition, chronic pain induction increased TRPV1 signaling pathway and correlated kinases in the mouse Hypo and CB. Furthermore, ACE and *TRPV1* gene deletion dramatically reduced these molecular changes, suggesting that TRPV1-induced central sensitization can be reversed.

5. Conclusions

We demonstrate that the antinociceptive effect of ACE is dependent on TRPV1 pathway in the mouse brain and that TRPV1 signaling pathways participated in pain control in the FM model (Fig. 6). We thereby propose that these could be possible novel targets for the management of chronic pain.

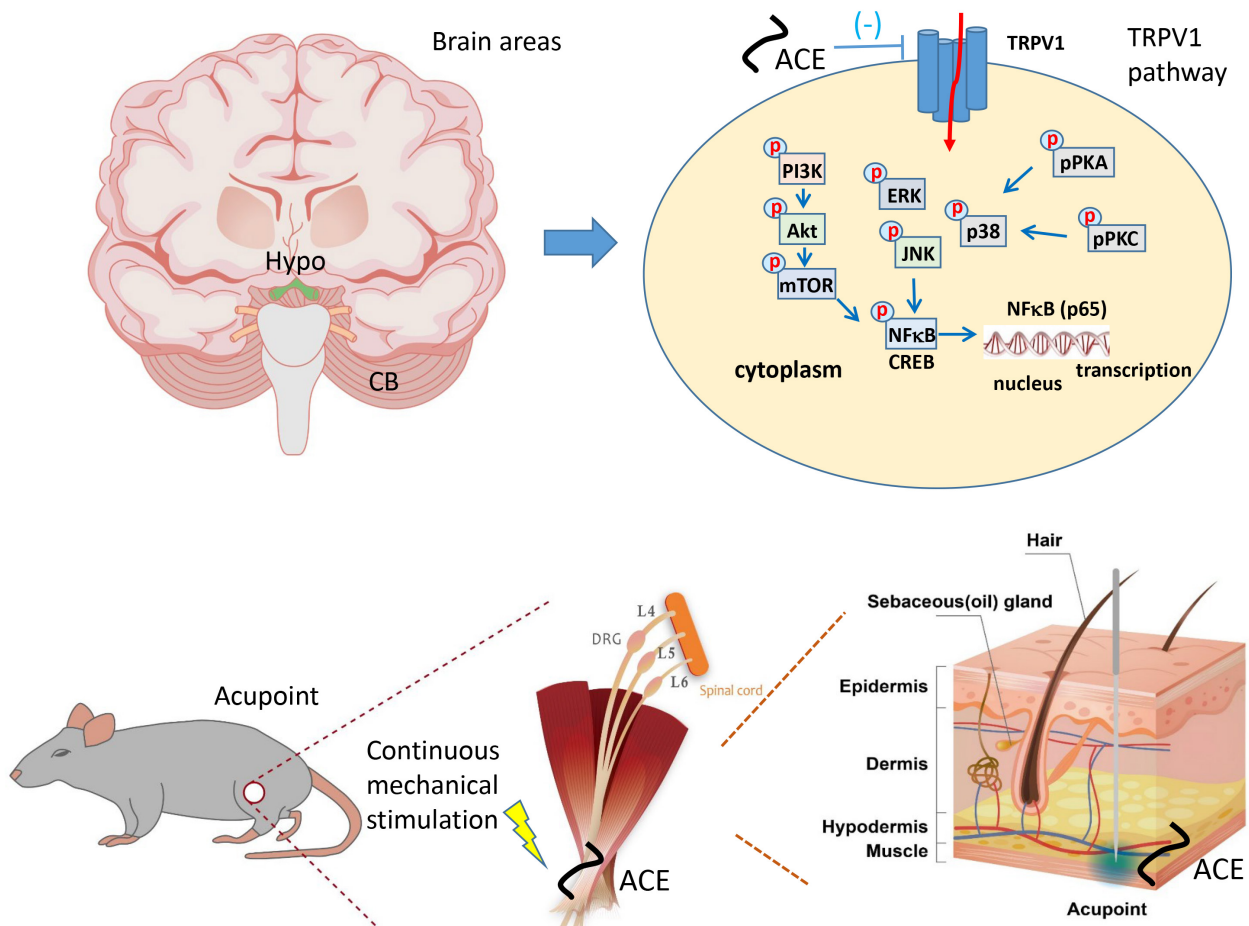


Fig. 6. Schematic diagram of TRPV1 and related factors altered by ACE. The summary picture shows the crucial effect of analgesic mechanisms involving TRPV1 and related factors in mice FM pain. ACE or *Trpv1*^{-/-} can significantly attenuate the overexpression of TRPV1 signaling pathway in the mice brain.

Abbreviations

CNS, central nervous system; ACE, Acupoint catgut embedding; TRPV1, Transient receptor potential vanilloid 1; FM, fibromyalgia; ICS, intermittent cold stress; WPI, widespread pain index; SS, symptom severity scale; Hypo, hypothalamus; CB, cerebellum; PKA, protein kinase A; PI3K, phosphoinositide 3-kinases; CaMKII, Ca²⁺/calmodulin-dependent kinase II; MAPK, mitogen-activated protein kinase; CREB, cAMP-response element binding protein; NFκB, nuclear factor kappa-light-chain-enhancer of activated B cells; SSC, somatosensory cortex; ACC, anterior cingulate cortex.

Availability of Data and Materials

The data used to support the findings of this study are available from the corresponding author upon request.

Author Contributions

PCL, CMY, and IHH performed the experiments, analyzed and interpreted the data, and wrote the draft

manuscript. YHC advice on the Western blot and ELISA experiments. YWL analyzed the data and draw the figures. YHC and YWL designed the research study and revised and submitted the manuscript. All authors contributed to editorial changes in the manuscript. All authors read and approved the final manuscript. All authors have participated sufficiently in the work and agreed to be accountable for all aspects of the work.

Ethics Approval and Consent to Participate

The treatment of mice was permitted by China Medical University Committee (CMUIACUC-2022-424), Taiwan, subsequent the guideline for the practice of experimental animals (National Academy Press).

Acknowledgment

The authors would like to thank Enago (<https://www.enago.tw/>) for the English language review.

Funding

This research was funded by Tzu Chi University TTCRD112-14, China Medical University CMU111-S-25, and the “Chinese Medicine Research Center, China Medical University” from The Featured Areas Research Center Program within the framework of the Higher Education Sprout Project by the Ministry of Education (MOE) in Taiwan.

Conflict of Interest

The authors declare no conflict of interest.

References

- [1] Delorme J, Kerckhove N, Authier N, Pereira B, Bertin C, Chenaf C. Systematic Review and Meta-Analysis of the Prevalence of Chronic Pain Among Patients With Opioid Use Disorder and Receiving Opioid Substitution Therapy. *Journal of Pain*. 2023; 24: 192–203.
- [2] Fitzcharles MA, Ste-Marie PA, Goldenberg DL, Pereira JX, Abbey S, Choinière M, et al. 2012 Canadian Guidelines for the diagnosis and management of fibromyalgia syndrome: executive summary. *Pain Research and Management*. 2013; 18: 119–126.
- [3] Häuser W, Ablin J, Perrot S, Fitzcharles MA. Management of fibromyalgia: practical guides from recent evidence-based guidelines. *Polish Archives of Internal Medicine*. 2017; 127: 47–56.
- [4] Marques AP, Santo ASDE, Berssaneti AA, Matsutani LA, Yuan SLK. Prevalence of fibromyalgia: literature review update. *Revista Brasileira de Reumatologia English Edition*. 2017; 57: 356–363.
- [5] Silveira MJ, Boehnke KF, Clauw D. Treatment of Fibromyalgia in the 21st Century. *JAMA Internal Medicine*. 2021; 181: 1011.
- [6] Shergis JL, Ni X, Jackson ML, Zhang AL, Guo X, Li Y, et al. A systematic review of acupuncture for sleep quality in people with insomnia. *Complementary Therapies in Medicine*. 2016; 26: 11–20.
- [7] You J, Li H, Xie D, Chen R, Chen M. Acupuncture for Chronic Pain-Related Depression: A Systematic Review and Meta-Analysis. *Pain Research and Management*. 2021; 2021: 6617075.
- [8] Hsu HC, Hsieh CL, Lee KT, Lin YW. Electroacupuncture reduces fibromyalgia pain by downregulating the TRPV1-pERK signalling pathway in the mouse brain. *Acupuncture in Medicine*. 2020; 38: 101–108.
- [9] Hsu HC, Hsieh CL, Wu SY, Lin YW. Toll-like receptor 2 plays an essential role in electroacupuncture analgesia in a mouse model of inflammatory pain. *Acupuncture in Medicine*. 2019; 37: 356–364.
- [10] Lin YW, Chou AIW, Su H, Su KP. Transient receptor potential V1 (TRPV1) modulates the therapeutic effects for comorbidity of pain and depression: The common molecular implication for electroacupuncture and omega-3 polyunsaturated fatty acids. *Brain, Behavior, and Immunity*. 2020; 89: 604–614.
- [11] Yen CM, Wu TC, Hsieh CL, Huang YW, Lin YW. Distal Electroacupuncture at the LI4 Acupoint Reduces CFA-Induced Inflammatory Pain via the Brain TRPV1 Signaling Pathway. *International Journal of Molecular Sciences*. 2019; 20: 4471.
- [12] Yen LT, Hsieh CL, Hsu HC, Lin YW. Preventing the induction of acid saline-induced fibromyalgia pain in mice by electroacupuncture or APETx2 injection. *Acupuncture in Medicine*. 2020; 38: 188–193.
- [13] Inprasit C, Huang YC, Lin YW. Evidence for acupoint catgut embedding treatment and TRPV1 gene deletion increasing weight control in murine model. *International Journal of Molecular Sciences*. 2020; 45: 779–792.
- [14] Zhong G, Yin X, Li J, Li X, Zhang Q. Acupoint catgut embedding for chronic low back pain: A protocol for systematic review and meta-analysis. *Medicine*. 2022; 101: e32409.
- [15] Guo M, Le X, Qin-Yu W, Ye M, Sheng-Qiang Z, Yao X, et al. Effectiveness and Safety of Acupoint Catgut Embedding for the Treatment of Poststroke Constipation: A Systematic Review and Meta-Analysis. *Evidence-Based Complementary and Alternative Medicine*. 2022; 2022: 8080297.
- [16] Zhou M, Yuan Y, Lin Z, Zhang B, Qin W, Liu Y, et al. Acupoint catgut embedding improves senescence in a rat model of ageing by regulating mitophagy via the PINK1 pathway. *Journal of Cellular and Molecular Medicine*. 2021; 25: 3816–3828.
- [17] Wang J, Lu S, Yang F, Guo Y, Chen Z, Yu N, et al. The role of macrophage polarization and associated mechanisms in regulating the anti-inflammatory action of acupuncture: a literature review and perspectives. *Chinese Medicine*. 2021; 16: 56.
- [18] Pei X, Song S, Li H, Lu D. Efficacy and safety of acupoint catgut embedding in treating postoperative pain of mixed hemorrhoids: A randomized controlled trial protocol. *Medicine*. 2021; 100: e25948.
- [19] Gao M, Wang Y, Liu L, Qiao Z, Yan L. A patent review of transient receptor potential vanilloid type 1 modulators (2014–present) Expert Opinion on Therapeutic Patents. 2021; 31: 169–187.
- [20] Liao H, Lin Y. Electroacupuncture reduces cold stress-induced pain through microglial inactivation and transient receptor potential V1 in mice. *Chinese Medicine*. 2021; 16: 43.
- [21] Hsiao IH, Liao HY, Lin YW. Optogenetic modulation of electroacupuncture analgesia in a mouse inflammatory pain model. *Scientific Reports*. 2022; 12: 9067.
- [22] Hsiao I, Lin Y. Electroacupuncture Reduces Fibromyalgia Pain by Attenuating the HMGB1, S100B, and TRPV1 Signalling Pathways in the Mouse Brain. *Evidence-Based Complementary and Alternative Medicine*. 2022; 2022: 2242074.
- [23] Bonanni R, Gino Grillo S, Cariati I, Tranquillo L, Iundusi R, Gasbarra E, et al. Osteosarcopenia and Pain: Do We Have a Way Out? *Biomedicines*. 2023; 11: 1285.
- [24] Lin T, Gargya A, Singh H, Sivanesan E, Gulati A. Mechanism of Peripheral Nerve Stimulation in Chronic Pain. *Pain Medicine*. 2020; 21: S6–S12.
- [25] Helm S, Shirsat N, Calodney A, Abd-Elsayed A, Kloth D, Soin A, et al. Peripheral Nerve Stimulation for Chronic Pain: A Systematic Review of Effectiveness and Safety. *Pain and Therapy*. 2021; 10: 985–1002.
- [26] Gilmore C, Ilfeld B, Rosenow J, Li S, Desai M, Hunter C, et al. Percutaneous peripheral nerve stimulation for the treatment of chronic neuropathic postamputation pain: a multicenter, randomized, placebo-controlled trial. *Regional Anesthesia and Pain Medicine*. 2019; 44: 637–645.
- [27] Koetsier E, Franken G, Debets J, Heijmans L, van Kuijk SMJ, Linderth B, et al. Mechanism of dorsal root ganglion stimulation for pain relief in painful diabetic polyneuropathy is not dependent on GABA release in the dorsal horn of the spinal cord. *CNS Neuroscience and Therapeutics*. 2020; 26: 136–143.
- [28] Nakashima C, Ishida Y, Kitoh A, Otsuka A, Kabashima K. Interaction of peripheral nerves and mast cells, eosinophils, and basophils in the development of pruritus. *Experimental Dermatology*. 2019; 28: 1405–1411.
- [29] Bonaz B, Sinniger V, Pellissier S. Targeting the cholinergic anti-inflammatory pathway with vagus nerve stimulation in patients with Covid-19? *Bioelectronic Medicine*. 2020; 6: 15.
- [30] Cui WQ, Sun WS, Xu F, Hu XM, Yang W, Zhou Y, et al. Spinal Serotonin 1a Receptor Contributes to the Analgesia of Acupoint Catgut Embedding by Inhibiting Phosphorylation of the N-Methyl-d-Aspartate Receptor GluN1 Subunit in Complete Freund’s Adjuvant-Induced Inflammatory Pain in Rats. *Journal of Pain*. 2019; 20: 16.e1–16.e16.
- [31] Du K, Wang X, Chi L, Li W. Role of Sigma-1 Receptor/p38 MAPK Inhibition in Acupoint Catgut Embedding-Mediated Analgesic Effects in Complete Freund’s Adjuvant-Induced Inflammatory Pain. *Anesthesia and Analgesia*. 2017; 125: 662–669.